PHYSICAL REVIEW D **95,** 034012 (2017)

NLO corrections to c- and b-quark fragmentation into j/ψ and γ

R. Sepahvand[*] and S. Dadfar[†]

Physics Department, University of Lorestan, 68151-44316 Khoramabad, Iran

(Received 28 September 2016; published 13 February 2017)

We present the next-to-leading-order (NLO) corrections to the fragmentation process of a heavy quark to a $^3S_1$ wave heavy quarkonium. The virtual and real corrections are calculated by using the dimensional regularization method. The divergences due to virtual NLO corrections are analytically extracted then we explain how the poles from phase-space integrals and from loop integrals are canceled by renormalization. We use the eikonal scheme to evaluate the soft real corrections in $4-2\varepsilon$ dimensions. Our numerical calculations show the fragmentation function (FF) at NLO is dependent on both the μ scale and the initial quark energy. These corrections have a significant effect on the shape and probability of the FF.

DOI: 10.1103/PhysRevD.95.034012

I. INTRODUCTION

Ever since the discovery of the j/ψ meson in 1974 [1] and subsequently Υ in 1977 [2], a long-term effort has been made, both experimentally and theoretically, to understand their production in hadronic collisions. Due to the inherent characteristics of j/ψ and Υ, in the family of heavy mesons, the study of heavy quarkonium may improve our knowledge of the standard model and of perturbative and nonperturbative quantum chromodynamics (QCD). The observation of quarkonium states j/ψ and Υ, from experimental data, is also one of the most famous identification tools of the quark gluon plasma signals [3].

In quarkonium physics, much of the theoretical progress is stimulated by experimental results obtained from the LHC and Tevatron accelerators. Recently, there have been new investigations of j/ψ and Υ meson production using pp collision data taken at high energies, from 2.76 to 7 TeV, by the LHCb [4–6], ALICE [7–9], ATLAS [10,11], and CMS [12–14] collaborations. The first measurement of quarkonium production has been presented with the LHCb detector at $\sqrt{s} = 8$ TeV by assumption of zero polarization [15]; moreover, both direct and indirect production of heavy quarkonium has also been analyzed in various other processes such as electron-positron annihilation, Z^o and B decays, and hadronic collisions at fixed-target experiments [16–20].

From theoretical and experimental perspectives, the partonic fragmentation is an important and arguable issue in the understanding of j/ψ and Υ meson production. Most of the studies on their production have been done by singlet color [21,22] and octet color models within nonrelativistic quantum chromodynamics (NRQCD) [23]. But the performed investigations between theoretical predictions and experiments have shown that none of these models can completely explain the polarization and transverse momentum.

In an effort to solve these problems, several approaches have been proposed. The FF for the splitting of partons into heavy quarkonium has been calculated using perturbative quantum chromodynamics (PQCD) [24,25] at the scale $\mu = 2m_Q$. The authors have summed up leading logarithms of μ/m_Q (μ and m_Q are factorization scale and heavy quark mass, respectively) by using the Altarelli-Parisi evolution equations. Most recently, the gluon FF into the $^1S_0$ quarkonium has been calculated by considering one-loop corrections [26]. Also, the relativistic corrections of the gluon FF into the $c\bar{c}$ pseudoscalar state has been computed by using that method [27]. In a study on the charm quark fragmentation into the S-wave quarkonium states, Ma [28] presented an approach that allows one to do systematic investigation on the higher-order corrections, as was illustrated in [29]. One-loop corrections and the QCD radiative corrections in α_s and relativistic velocity ν lead to an increase in the cross section of quarkonium production in the case of S-wave states. Recently, heavy quarkonium FFs at the input scale, $\mu > 2m_Q$, have been calculated in terms of the NRQCD factorization approach in its velocity expansion for the S and P waves states [30].

We apply the NLO corrections on the fragmentation of the heavy quark into the $^3S_1$ states of quarkonium, j/ψ and Υ. We should note that complete evaluation of the scattering processes at NLO in QCD requires the calculation of leading-order graphs, virtual corrections, and real gluon emission contributions. The results of this work may be used in the calculation of cross sections.

This text is organized as follows: In Sec. II, the FF of the c quark to heavy meson is algebraically calculated at LO in α_s. A more complete discussion can be found in Ref. [31]. In Sec. II, a general description of the NLO calculations is given by using the dimensional regularization technique. As is well known, this technique is the most appropriate method for regulating UV and IR divergences. For the two parts of the virtual and real corrections, we use this approach to calculate the NLO corrections at the

[*]r.sepahvand@gmail.com
[†]dadfar.sa@fs.lu.ac.ir

fragmentation process. In the last section, we summarize the procedure of our calculations then analyze the numerical results at the LO and NLO accuracy for the scales $\mu_0 > 2m_Q$.

II. FRAGMENTATION FUNCTION AT LEADING ORDER

The fragmentation process of heavy quark to quarkonium, $Q(p_2) \to Q\bar{Q}(p) + Q(k_2)$, at lowest order in α_s, corresponds to the Feynman diagram as shown in Fig. 1. We have assumed that the momentum of the final meson is assigned as $p = p_1 + k_1$, such that $Q(p_1)$ and $\bar{Q}(k_1)$ are emitted collinearly with each other. The four momenta are labeled in Fig. 1.

By using NRQCD factorization, the fragmentation function can be formulated as a power series in α_s as the following form:

$$\begin{aligned} \mathrm{D}^{Q\to Q\bar{Q}}(z) &= \langle \mathrm{O}_1(^1\mathrm{S}_0)\rangle^{Q\bar{Q}}[\alpha_s^2 d_{\mathrm{LO}}(z) + \alpha_s^3 d_{\mathrm{NLO}}(z) + \cdots] \\ &= \mathrm{D}_{\mathrm{LO}} + \mathrm{D}_{\mathrm{NLO}}. \end{aligned} \tag{1}$$

The matrix element $\mathrm{O}_1(^1\mathrm{S}_0)^{Q\bar{Q}}$ is a proportional color-singlet common projection operator [26]. So far, different methods have been used to calculate the quark FF at LO based on Suzuki [32], Collins [33], Braaten [24], etc. The final result of their functions is gauge invariance. The initial conditions of our calculations at LO are the same as Ref. [31], but there are differences in the method of calculation of the phase-space integrals and amplitude. The FF at LO can be briefly expressed in following standard form:

$$\mathrm{D}_{\mathrm{LO}}(\mathrm{z}) = N \int |\mathrm{M}_{\mathrm{LO}}|^2 \mathrm{dPS}_2, \tag{2}$$

where z is the longitudinal energy–momentum fraction of the meson and M_{LO} is the amplitude at LO. N may be obtained by a normalization condition of the FFs. dPS_2 stands for the differential of the two-body phase space which can be expressed as

$$\mathrm{dPS}_2 = \frac{1}{(2\pi)^3}\frac{\mathrm{d}^3\vec{p}\,\mathrm{d}^3\vec{k}_2}{4p^0k_2^0}\delta^3(\vec{p}_2 - \vec{k}_2 - \vec{p}), \tag{3}$$

$$\begin{aligned} &\int \mathrm{dPS}_2(Q(p_2) \to H(p) + Q(k_2)) \\ &\quad = \int \frac{1}{4}\frac{1}{(2\pi)^3}\frac{1}{p^0}\frac{\mathrm{d}^3k_2}{k_2^0}\delta(p_2^0 - p^0 - k_2^0), \end{aligned} \tag{4}$$

where $\mathrm{d}^3k_2 = k_2^0\mathrm{d}^2k_2^T$ and $p_2^0 = \sqrt{s_1}$. We assume that the meson and final quark form two- body phase space. The LO amplitude for hadronic production can be written as

$$\mathrm{M}_{\mathrm{LO}}(p,p_2,k_2) = \frac{v(k_1)\bar{u}(p_1)}{(k_1+k_2)^2} ig\gamma_\mu \frac{\lambda^a}{2}\frac{\not{p}_2 + m_Q}{p_2^2 - m_Q^2} ig\gamma_\mu \frac{\lambda^b}{2} u(k_2). \tag{5}$$

The overall color factor is C_F^2. In the Feynman gauge, $\frac{\lambda^i}{2}$ is the generator of the SU(3) representation. The common projection operator is defined as follows:

$$\begin{aligned} v(k_1,s)\ \bar{u}(\mathrm{p}_1,s) &= \frac{\psi_{\mathrm{M}}(0)}{2\sqrt{2}m^{3/2}}(\not{p}_1 + m)\not{\varepsilon}(p)(\not{k}_1 + m) \\ &\quad \otimes \left(\frac{1_c}{\sqrt{N_c}}\right), \end{aligned} \tag{6}$$

where $\not{\varepsilon}(\mathrm{p})$ is the polarization vector for vector states j/ψ (Υ), 1_c and N_c stand for the unit color matrix and the number of color, $N_c = 3$ for QCD, and $C_F = (N_c^2 - 1)/2N_c$ is color factor. $\psi_M(0)$, a nonperturbative parameter, is a Schrödinger wave function at the origin of the $j/\psi(\Upsilon)$ meson with $M = 2m_Q$ ($Q = c$ and b quarks). The fraction of the initial quark's momentum, z, is transferred to a heavy quark-antiquark system and each component carries a fraction of x_1, x_2 and the final quark takes the remaining

$$z = \frac{E_{\mathrm{Meson}}}{E_{\mathrm{Quark}}} = \frac{p^0}{p_2^0}. \tag{7}$$

The four momenta of the particles are parametrized as

$$p^0 = zp_2^0,\ \ p_1^0 = x_1 z p_2^0,\ \ k_1^0 = x_2 z p_2^0,\ \ k_2^0 = (1-z)p_2^0. \tag{8}$$

By applying the fragmentation kinematics and the scalar product of four vectors, and integrating over the final-state phase space as obtained in Ref. [31,34], we can obtain FF at LO as

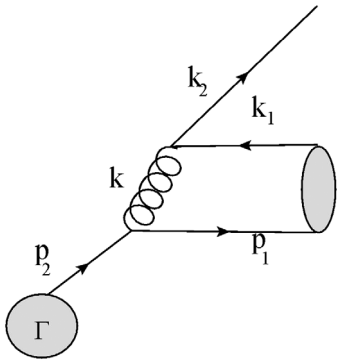

FIG. 1. The Feynman diagram at LO for quarkonium production at the quark fragmentation process.

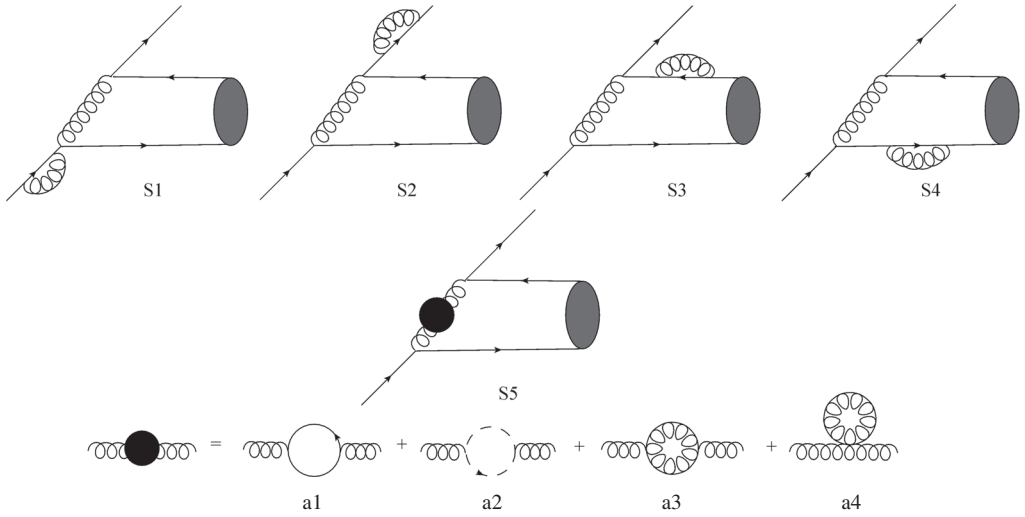

FIG. 2. The self-energy diagrams.

$$D(z)_{\mathrm{LO}} = \frac{-2\alpha_s^2 C_F^2 r|\Psi_M(0)|^2}{27\pi\xi(z)m_2^3(z-1)z}[(r^2+42r+41)z^4 - 8(17r+1)z^3 + 8(17r+3)z^2 - 32z + 16], \tag{9}$$

where in the fragmentation function, $\xi(z)$ and r are

$$\xi(z) = -\frac{((r+1)z^2-4z+4)^3}{16(z-1)^3z^2}, \qquad r = k_T'^2/m_Q^2, \tag{10}$$

where k_T' is equal to the transverse momentum of the initial heavy quark which is only carried by the final state heavy quark at LO, $p_{2T} = k_{2T} = k_T'$, and the term $\alpha_s(2m_Q)$ is the strong interaction coupling constant. We have calculated this diagram in the Feynman gauge and the results are the same as Ref. [24] which have been worked in light cone gauge. Our calculation at LO is gauge invariant, and it is close to Eq. (16) in Ref. [24]. Finally, the total FP and average fraction of longitudinal energy momentum, for the production of the S-wave bound state, are defined as

$$\mathrm{FP} = \int_0^1 \mathrm{D}(z)_{\mathrm{LO}}\mathrm{d}z, \tag{11}$$

$$\langle z\rangle = \frac{\int_0^1 z \times \mathrm{D}_{\mathrm{LO}}(z)\mathrm{d}z}{\int_0^1 D_{\mathrm{LO}}(z)\mathrm{d}z}. \tag{12}$$

III. NEXT-TO-LEADING-ORDER CORRECTIONS

The NLO corrections of the heavy quark fragmentation to quarkonium include the contributions of virtual and real QCD corrections. Typical Feynman diagrams which contribute to the one-loop corrections at the fragmentation process of a heavy quark into j/ψ and Υ mesons are shown in Figs. 2–5. For the two kinds of vertices, $g \to b\bar{b}$ and $c \to c\bar{c}$, we need only consider one of them sincethey are similar.

The amplitude of NLO corrections, $\mathrm{M_{NLO}}$, is a combination of the contributions of virtual and real corrections. First, we focus on the calculation of virtual corrections. The virtual corrections amplitude, $\mathrm{M_{Virtual}}$, contains the corrections of the self-energy according to Fig. 2, triangle diagrams, Fig. 3, and box diagrams, Fig. 4. The sum over helicities and colors is performed for each loop diagram separately. The virtual corrections amplitude, $\mathrm{M_{virtual}}$, is calculated according to the typical structure of Fig. 5,

$$|\mathrm{M_{virtual}}|^2 = \mathrm{M}^L\mathrm{M}^R. \tag{13}$$

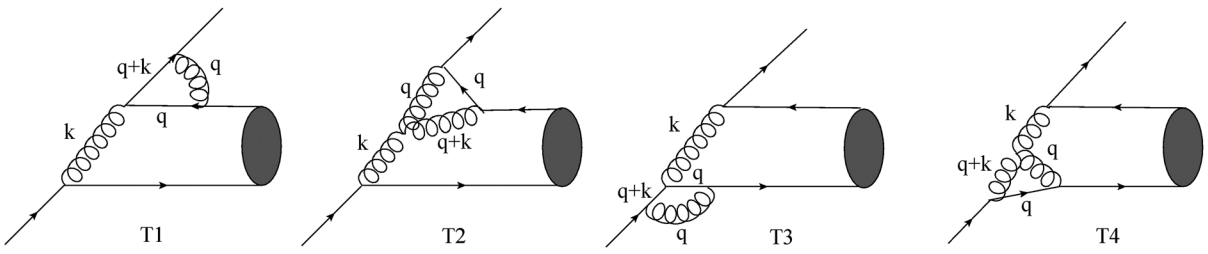

FIG. 3. The triangle diagrams in the virtual correction.

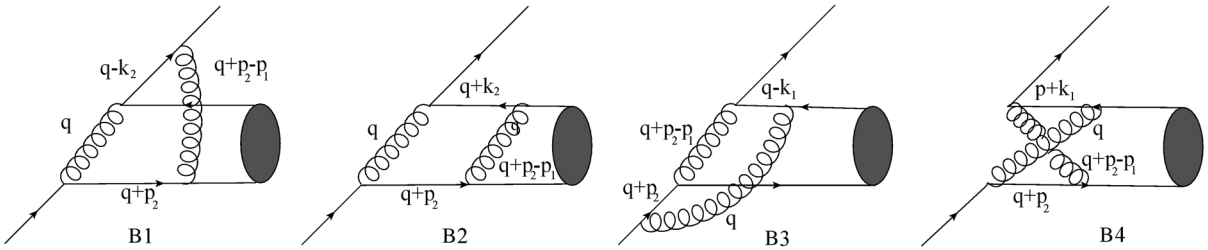

FIG. 4. The box diagrams in the virtual correction.

The M^L amplitude in the left side of the cut is coupled to M^R, the amplitude in the right side of the cut, with an eikonal line.

For all diagrams, we should first write M^L, which is the part of the scattering amplitude containing one-loop corrections in the left side of cut of Fig. 5. The self-energy corrections for S1 in Fig. 2 are written in the following form [35]:

$$M^L_{S1} = \frac{\not{p}_2 + m_Q}{p_2^2 - m_Q^2}\,\Pi_{S1}\, ig_s\gamma_\mu\frac{\lambda^b}{2}\,\frac{v(k_1)\bar{u}(p_1)}{(k_1+k_2)^2}\,ig_s\gamma_\mu\frac{\lambda^a}{2}\,u(k_2) \tag{14a}$$

$$\Pi_{S1} = \frac{1}{3}\int\frac{d^4q}{(2\pi)^4}\gamma_\nu\frac{\not{q}_1}{q_1^2 - m_Q^2 + i\varepsilon}\gamma_\sigma\frac{1}{q^2-\lambda^2+i\varepsilon},$$
$$q_1 = p_2 - q. \tag{14b}$$

The self- energy tensor, Π, for S2, S3, and S4, is similar to S1 except that q_1 is not identical in its formalism. In S5, the corrections of the fermion, ghost, and gluon loops to the gluon propagator are shown. The sum over the ghost and gluon loop is gauge invariant. The tensor formalisms of vacuum polarization S5 are given in the below forms,

$$\Pi_{S5} = \frac{C_F\alpha_s}{4\pi}\left(\frac{1}{\varepsilon_{uv}} - \log\frac{-k^2}{\mu^2}\right)\left(\frac{1}{5} - \frac{2}{3}n_f\right)(g_{\mu\nu}k^2 - k_\mu k_\nu), \tag{15}$$

where Γ_{S5} is the spinor amplitude that contains the contributions of the propagator corrections and n_f is the number of quark flavors. For all diagrams, the conservation of the vector current can be guaranteed by writing down the amplitudes starting from the identical vertex. The triangle diagrams corresponding to the QCD vertex are shown in Fig. 3. In the Feynman gauge, the contribution of the vertex corrections is

$$M^L_{T1} = \frac{\not{p}_2 + m_Q}{p_2^2 - m_Q^2}\,\Pi_{T1}\, ig\gamma_\mu\,\frac{g_{\mu\rho}v(k_1)\bar{u}(p_1)}{(k_1+k_2)^2}\,u(k_2) \tag{16a}$$

$$\Pi_{T1} = g^3\int\frac{d^4q}{(2\pi)^4}\frac{\lambda^b}{2}\gamma^\nu\frac{\lambda^a}{2}\frac{(\not{q}+m_Q)}{(q^2-m_Q^2+i\varepsilon)} \times\gamma_\rho\frac{(\not{q}+\not{k}+m_Q)}{((q+k)^2-m_Q^2+i\varepsilon)}\frac{\lambda^c}{2}\gamma_\sigma\frac{1}{(q^2-\lambda^2+i\varepsilon)} \tag{16b}$$

$$M^L_{T2} = \frac{\not{p}_2 + m_Q}{p_2^2 - m_Q^2}\,ig\gamma_\mu\,\frac{g_{\mu\rho}v(k_1)\bar{u}(p_1)}{(k_1+k_2)^2}\,\Pi_{T2}u(k_2) \tag{17a}$$

$$\Pi_{T2} = -g^3\int\frac{d^4q}{(2\pi)^4}f^{abc}\gamma_\rho[g_{\rho\sigma}(k-q)_\nu + g_{\nu\rho}(-q-2k)_\sigma + g_{\sigma\nu}(2q+k)_\rho]\frac{\lambda^b}{2}\frac{\lambda^c}{2}\gamma_\nu \times\frac{(\not{q}+m_Q)}{(q^2-m_Q^2+i\varepsilon)(q^2-\lambda^2+i\varepsilon)((q+k)^2-\lambda^2+i\varepsilon)}\gamma_\sigma. \tag{17b}$$

Γ_{Ti} is considered the vertex correction related to the triangle diagram Ti (i = 1, 2,3,4). The triangle tensors of T3 and T4 are written in the same manner as T1 and T2. The structure constant of the SU (3) group is displayed with f^{abc}. γ_σ which appears in calculation of Π_{Ti} incorporated into the vector current Γ_{Ti}. The other corrections of NLO are according to the box diagrams, B1 and B2, as follows:

$$\mathrm{M}^{L}_{\mathrm{B1}} = g^4 \int \frac{\mathrm{d}^4 q}{(2\pi)^4} \frac{\not p_2 + m_Q}{p_2^2 - m_Q^2} \gamma^\mu \frac{(\not q + \not p_2 + m_Q)}{((q+p_2)^2 - m_Q^2 + i\varepsilon)} \frac{u(p_1)\bar{\mathrm{v}}(k_1)}{(k_1+k_2)^2} \gamma_\nu \frac{g_{\rho\mu}}{(q+p_2-p_1)^2 + i\varepsilon},$$
$$\times \gamma_\rho \frac{(\not q - \not k_2 + m_Q)}{((q-k_2)^2 - m_Q^2 + i\varepsilon)} \gamma_\sigma u(k_2) \frac{g_{\sigma\nu}}{(q^2 - \lambda^2 + i\varepsilon)}, \tag{18}$$

and

$$\mathrm{M}^{L}_{\mathrm{B2}} = g^4 \int \frac{\mathrm{d}^4 q}{(2\pi)^4} \frac{\not p_2 + m_Q}{p_2^2 - m_Q^2} \gamma^\mu \frac{(\not q + \not p_2 + m_Q)}{((q+p_{21})^2 - m_Q^2 + i\varepsilon)} \gamma_\nu \frac{g_{\rho\mu}}{(q+p_2-p_1)^2 + i\varepsilon},$$
$$\times \gamma_\rho \frac{u(p_1)\bar{\mathrm{v}}(k_1)}{(k_1+k_2)^2} \frac{(\not q + \not k_2 + m_Q)}{((q+k_2)^2 - m_Q^2 + i\varepsilon)} \gamma_\sigma u(k_2) \frac{g_{\sigma\nu}}{(q^2 - \lambda^2 + i\varepsilon)}. \tag{19}$$

By considering the kinematic illustrated in the diagrams, the box tensors of B3 and B4 are written in the same manner as B1 and B2. Although B4 apparently has a different topology, its formalism is simply written by renaming the quark lines. For the tensor integral solution of the vertex and box corrections, we use the three- and four-point scalar integrals, respectively. In all equations, the mass of the heavy quarks is nonzero. We have calculated the integrals with one- two-, and three-point Feynman propagators and an eikonal propagator by using the useful integrals in Appendix B of Ref. [26].

Since M^R in the virtual corrections has no divergences, in $\varepsilon = 0$, $\mathrm{M_{LO}}$ is used instead of M^R. The rules for the right of the cut are conjugate of the rules on the left side. In calculations, the term $i/(\not p_2 - m_Q)$ comes from coupling the initial quark coupled to the eikonal line. According Feynman rules for diagrams that contain the eikonal line, each eikonal-line propagator with momentum ℓ, contributes a factor $i/(\ell - \not m) \to i\delta_{ij}/(\ell.n)$ where i and j are color indices. In Refs. [30,33,34], the usefule rules have been stated for the Feynman diagrams that lie to the left and right of the final-state cut.

These integrals are divergent for large values of the internal loop momenta; thus, we have first to regularize them by using the method of dimensional regularization with $D = 4 - 2\varepsilon$, then we cancel the infinities by renormalization.

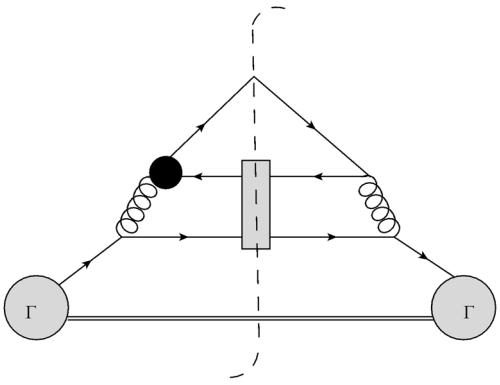

FIG. 5. Typical structures of the amplitudes squared of virtual corrections.

In our calculation, FeynArts [36] is used to plot the Feynman diagrams. The algebraic calculations like tensor algebra, tensor integral decomposition, and reduction and trace are done by Mathematica package FeynCalc [37]. For the numerical evaluation of Feynman diagrams, we have written some codes in maple. So, we limit ourselves to presenting the results of the calculation of the one-loop corrections in the fragmentation process at NLO for Figs. 2–5.

In the output of our calculation, we find terms contained in ε^{-1} which express the divergent part. The regularization of FF is done in terms of the quark and gloun fields, the strong coupling constant g, and the heavy quark mass m. The renormalization of the coupling constant is performed in the minimal-subtraction (MS) scheme, whereas the renormalization of heavy quark mass and quark field is done in the on-shell (OS) mass scheme. The counterterms of $\delta Z_g^{\overline{MS}}$, δZ_2^{OS}, δZ_3^{OS} and δZ_m^{OS} have been presented in Ref. [38]. According to the power-counting rules, all UV divergences appearing in vacuum polarization and the triangle and box diagrams are removed by the counterterms (CTs) of the external parton which form the quarkonium and the result is UV-free. δZ_2 and δZ_3 have IR poles. The eikonal counterterm is proportional to the quark field counterterm. The IR divergences of the FF in CTs have the following form:

$$\mathrm{D}(z)^{\mathrm{IR}}_{\mathrm{Counter}} \to -\frac{3\alpha_s C_F}{\pi \varepsilon_{\mathrm{IR}}} \mathrm{D_{LO}}(z). \tag{20}$$

It is removed after adding the IR divergences in the real and virtual NLO corrections. The IR divergences existing in virtual corrections are found in the box and triangle diagrams. The combination of virtual infrared divergences related to amplitude spinors is done as

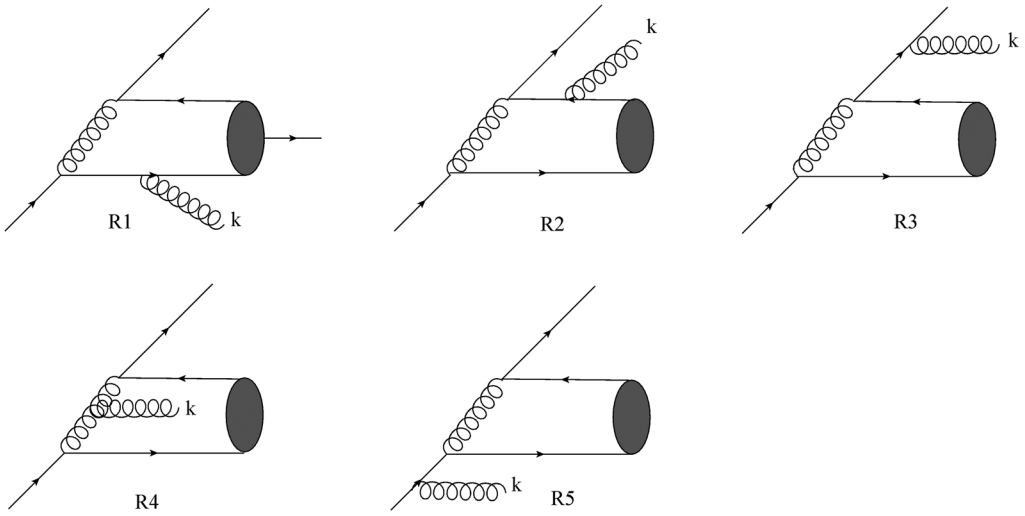

FIG. 6. The Feynman diagrams contain real corrections that contribute to the production of quarkonium.

$$\mathrm{M}^{\mathrm{IR}}_{\mathrm{Vitrual}} = \mathrm{M}^{\mathrm{IR}}_{\mathrm{Box}} + \mathrm{M}^{\mathrm{IR}}_{\mathrm{Triangle}}. \tag{21}$$

Among the triangle and box diagrams, we find that the IR divergence appearing in the T1 diagram is canceled by a similar divergence in the B1 diagram; in addition the combination of T3 and B3 is IR finite. B2 has both collinear singularities and IR divergence. The remaining IR divergences have the following form:

$$\mathrm{M}^{\mathrm{IR}}_{\mathrm{Virtual}} = \frac{3C_F\alpha_s}{4\pi}\frac{1}{\epsilon_{\mathrm{IR}}}\left(\frac{m_Q^2 - 2(p_2.p)x_s\log(x_s)}{(1-x_s^2)m_Q^2} + 1\right)\mathrm{M}_{\mathrm{LO}}, \tag{22}$$

where $x_s = -K(s_1, m_Q, m_Q)$ and $K = \left(1 - \sqrt{1-\frac{4m_Q^2}{s_1}}\right)/\left(1 + \sqrt{1-\frac{4m_Q^2}{s_1}}\right)$. $\sqrt{s_1}$ is the equal energy of the initial quark so that its value has to be $\sqrt{s_1} > 3m_Q$ for fragmentation at high transverse momentum at NLO. In Eq. (20), the last sentence is due to IR divergences in CTs. These divergences are canceled by their corresponding parts in real corrections. Therefore, the vitrual corrected FF can be expressed as

$$\mathrm{D}_{\mathrm{Vitrual}}(\mathrm{z}) = \mathrm{N}\int \mathrm{dPS}_2 |\mathrm{M}_{\mathrm{Vitrual}}|^2, \tag{23}$$

The calculations show that $\mathrm{M}_{\mathrm{Vitrual}}$ can be written as a combination of leading-order amplitude,M_{LO}, and the loop corrections amplitude. The FF in the sector real correction can be expressed as

$$\mathrm{D}_{\mathrm{Real}}(\mathrm{z}) = \mathrm{N}\int \mathrm{dPS}_3 |\mathrm{M}_{\mathrm{Real}}|^2, \tag{24}$$

where dPS_3 is the three-body phase space of final states in real correction. The Feynman diagram in real corrections is schematically shown in Figs. 6–7. In the eikonal approximation, the amplitude squared is obtained as

$$|\mathrm{M}_{\mathrm{Real}}|^2 = 4\pi\alpha_s |M_{\mathrm{LO}}|^2 \left(\frac{m_Q^2}{(k.k_2)^2} + \frac{m_Q^2}{(k.p_2)^2}\right), \tag{25}$$

Equation (25) contains the IR singularity. To regularize the IR singularities appearing in real corrections, we have employed the "Two cut off phase space slicing method" [39]. In this way, IR divergences are regularized by a cut on the energy of the emitted gluon. If the emitted gluon energy is considered $k_0 > \delta_s$, it is called hard, while $k_0 < \delta_s$ is treated as soft. The parameter δ_s has a small quantity in the energy unit. In real corrections, the amplitudes squared of the soft and hard energy have the same structure. Under the condition $k_0 < \delta_s$, the soft region, we have

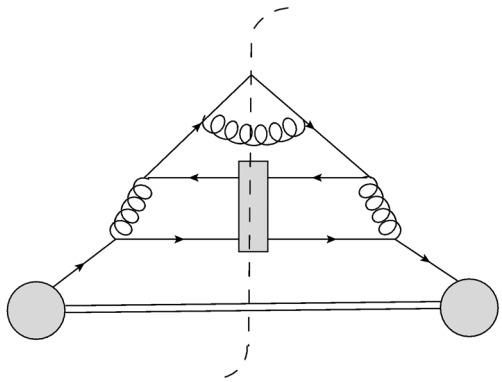

FIG. 7. Typical structure of the amplitudes squared of real corrections.

$$\mathrm{dPS}_3^{\mathrm{Soft}} = \mathrm{dPS}_2 \frac{\mathrm{d}^3k}{(2\pi)^3 2k_0}\bigg|_{k_0<\delta_s}. \tag{26}$$

The three-body phase space for the real correction in the hard region can be expressed as

$$\mathrm{dPS}_3^{\mathrm{Hard}} = \frac{1}{16(2\pi)^5}\frac{\mathrm{d}^3\vec{p}}{p_0}\frac{\mathrm{d}^3\vec{k}_2}{k_{20}}\frac{\mathrm{d}^3\vec{k}}{k_0}\delta^3(\vec{p}_2-\vec{p}-\vec{k}_2-\vec{k}) \times \delta(p_{20}-p_0-k_{20}-k_0) \tag{27}$$

$$\int \mathrm{d}^3\vec{p} = \int 4\pi p_0 \mathrm{d}p_0 \tag{28a}$$

$$\int \mathrm{d}^3\vec{k} = \int k_L \mathrm{d}^2k_T \tag{28b}$$

The kinematic for this scattering is obtaiend as

$$p = z(\sqrt{s_1}, 0, p_T, \sqrt{s_1}) \tag{29a}$$

$$p_2 = (\sqrt{s_1}, 0, p_{2T}, \sqrt{s_1}), \tag{29b}$$

$$k_2 = x(\sqrt{s_1}, 0, k_{2T}, \sqrt{s_1}), \tag{29c}$$

$$k = (1-z-x)(\sqrt{s_1}, 0, k_T, \sqrt{s_1}) \tag{29d}$$

The four-momentum energy conservation yields $(k+k_2)^2 = (p_2-p)^2$ and then $(k_2.k) = 2m_Q^2$. So, for the hard sector, we have

$$\int \mathrm{dPS}_3^{\mathrm{Hard}} |M_{\mathrm{Real}}|^2 = \iint \frac{{s_1}^2(1-z-x)z}{16(2\pi)^4 m_Q^2 x}\mathrm{d}z\mathrm{d}x, \tag{30}$$

where $0 \le z \le 1-\delta_s$, $1-\delta_c \le x \le 1+\delta_c-z$, and $\delta_c \ll \delta_s$ [39]. The result of the integrations over the hard phase space multiplied by the hard amplitude squared is a logarithmic function of the soft cutoff δ_s.

In the real corrections, the combination of R1 and R2 shows no IR singularities. R3 and R5 have IR collinear singularity, and R4 is IR finit. The sum of the soft and hard parts gives the full real correction. The collinear singularity and the IR divergence in the real corrections can be expressed as

$$\mathrm{M}_{\mathrm{Real}}^{\mathrm{IR}} = \frac{3C_F\alpha_s}{4\pi}\frac{1}{\varepsilon_{\mathrm{IR}}}\left(\frac{4}{3}\log(\delta_s) - \frac{m_Q^2 - 2(p_2.p)x_s\log(x_s)}{(1-x_s^2)} + 2\right) \times \mathrm{M}_{\mathrm{LO}} \tag{31}$$

$$M_{\mathrm{Collinear}}^{\mathrm{IR}} = -\frac{3C_F\alpha_s}{4\pi}\frac{1}{\varepsilon_{\mathrm{IR}}}\left(\frac{4}{3}\log(\delta_s) - 1\right) \times \mathrm{M}_{\mathrm{LO}}, \tag{32}$$

the $\log(\delta_s)$ involved in the terms that will be canceled by the δ-dependent terms in the hard sector of the real corrections. The combination of Eqs. (20) with, (22), (31), and (32) leads to removing IR divergences. All UV and IR divergences in the Feynman gauge are well defined and our calculation is gauge invariant. Finally, one can obtain the FF at NLO for the process $Q \to j/\psi(\Upsilon) + Q$ as

$$\mathrm{D}_{\mathrm{NLO}}(\mathrm{z}) = \int |M_{\mathrm{Soft}}|^2 \mathrm{dPS}_3^{\mathrm{Soft}} + \int |M_{\mathrm{Hard}}|^2 \mathrm{dPS}_3^{\mathrm{Hard}} + \int |M_{\mathrm{Virtual}}|^2 \mathrm{dPS}_2, \tag{33}$$

so that we have

$$\mathrm{D}(\mathrm{z}) = \mathrm{D}_{\mathrm{LO}}(\mathrm{z}) = \mathrm{D}_{\mathrm{NLO}}(\mathrm{z}). \tag{34}$$

The FF is obtained as a function of the quark mass, $s_{12} = (p_2-p_1)^2$, μ scale, logarithms of the soft δ_s, and collinear δ_c cutoffs. All terms of order δ_s and δ_c are neglected. Finally, we can compute them numerically.

IV. RESULTS AND DISCUSSION

In this work, the heavy quark FF to heavy quarkonium has been calculatd by applying one-loop corrections at process $Q \to Q\bar{Q} + Q$, where Q can be c and b quarks. We briefly reviewed the procedure used in our previous work [31] for the extraction of the nonperturbative FF at LO in α_s. They were finally described only with two parameters—longitudinal energy–momentum fraction z and the transverse momentum of the initial quark k_T. In order to achieve higher-order corrections, we calculated the FF according to Figs. 2–5. For the numerical calculations, the following input parameters are used:

$$m_c = 1.5\,\mathrm{GeV},\ \ m_b = 4.5\,\mathrm{GeV},\ \ \langle k_T^2\rangle_{j/\psi} = 0.7\,\mathrm{GeV}^2,$$
$$|\psi_\Upsilon(0)|^2 = 6.48\,\mathrm{GeV}^3,\ \ |\psi_{j/\psi}(0)|^2 = 0.81\,\mathrm{GeV}^3.$$

Here, $\Psi(0)$ is the value of the heavy meson's radial wave function at the origin [18]. For j/ψ and Υ, the FF at LO is close to the result in Ref. [32]. It agrees with Ref. [24] and is smaller than Ref. [34] by a factor $1/(2\mathrm{N}_c)$ in the limit $\varepsilon = 0$. The authors in Ref. [34] have followed the Collins-Soper model and have considered some additional diagrams. The eikonal line is part of the Collins and Soper set of rules, and it allows a gauge-invariant definition of the fragmentation function. But at the LO, one can avoid their definition and use another construction of the FF where it maintains gauge invariance. Thus, it can be concluded that our FF according to the Suzuki model at LO is gauge invariant. In the calculation of NLO corrections, eikonal lines have been used. First, the corrections of the amplitude at the NLO are calculated in the left side of the cut and then merged with the amplitude in the right side of the cut. The

TABLE I. The universal FP $\times 10^{-3}$ at LO and NLO for the j/Ψ and Υ mesons in the c and b quark fragmentation, respectively, at $\sqrt{s_1} = 2\mu$. The results of Eq. (18) in Ref. [40] have been divided to π.

LO		NLO	
Our work	0.18	$\mu = 3m_c$	0.21
[24]	0.18	$\mu = 5m_c$	0.22
[34]	1.13	$\mu = 10m_c$	0.23
[32,40]	0.14	$\mu = 10m_c$	0.35

NLO correction is done by the well-known method of dimensional regularization. The running strong coupling α_s is evaluated at one loop by evolving from the experimental value $\alpha_s(M_Z) = 0.11$, and it is given by

$$\frac{\alpha_s}{4\pi} = \frac{1}{\beta_0 L} - \frac{\beta_1 \log L}{\beta_0^3 L}, \tag{35}$$

where $\beta_0 = (33 - 2n_f)/4$, $\beta_1 = (34/3)C_A^2 - 4\,C_F T_F n_f - (20/3)\,C_A T_F n_f$, and $L = \log(\mu^2/\Lambda^2_{\rm QCD})$ with $\mu = 2m_Q$ and $\Lambda_{\rm QCD} = 166$ MeV. For the renormalization scales appearing in D(z), we adopt different renormalization scales in D(z), $\mu = 3m_Q$, $5m_Q$, $10m_Q$, and $30m_Q$. In the virtual corrections, we assumed that the initial heavy quark transverse momentum, k'_T, is carried by the final heavy quark with four-momentum k_2 and in the real corrections, it is distributed between the final quark and soft or hard gluon. In the real corrections, the finite terms of the virtual corrections are integrated over the two-body phase space. In the real corrections, the subtracted finite terms of the soft and hard amplitude are integrated over the phase space of the three final state. After cancellation of all divergences in the NLO corrections and adding all the finites, the total FF is obtained as Eq. (33). The FF at LO is dependent on the μ scale via the coupling constant while at NLO this dependence appears in both the coupling constant and NLO corrections, especially in virtual terms. In the NLO calculations, the initial quark energy should be larger than the initial scale for fragmentation, so we considered it to be at least 2 times the μ scale.

The total FPs have been listed in Tables I and II for production of j/Ψ and Υ mesons at NLO in μ different scales. The total FP is obtained by integrating the FF at NLO and LO over z from 0 to 1. As expected, the FP at NLO is larger than the FP at LO in different values μ. The numerical results listed in Tables I and II indicate that when renormalization scale μ increases NLO corrections dramaticaly enhance the FP. The initial quark energy has been considered as the function of μ, the growth of this scale increases energy of initial heavy quark for fragmentation to quarkonium so, the FP at NLO slowly increase. In Table III, the FPs have been evaluated with respect to variations of the initial quark energy.

TABLE II. The universal FP $\times 10^{-4}$ at the LO and NLO scale for the Υ meson in the b quark fragmentation at $\sqrt{s_1} = 2\mu$. The results of Eq. (18) in Ref. [40] have been divided to π.

LO		NLO	
Our work	0.38	$\mu = 3m_b$	0.44
[24]	0.33	$\mu = 5m_b$	0.45
[34]	2.1	$\mu = 10m_b$	0.47
[40]	0.26	$\mu = 10m_b$	0.69

TABLE III. The universal FP at the NLO level for the j/Ψ and Υ mesons in the c and b quark fragmentation, respectively, at the $\mu = 3m_Q$ scale for different values of $\sqrt{s_1}$.

$\sqrt{s_1}$	2μ	2μ	5μ	10μ	15μ
$F.P_{j/\Psi} \times 10^{-3}$	0.21	0.22	0.23	0.25	0.29
$F.P_{\Upsilon} \times 10^{-4}$	0. 38	0.45	0.47	0.52	0.60

The FFs of the j/Ψ and Υ mesons have been plotted in Figs. 8 and 9, respectively, in different scales μ from $\mu = 3m_Q$ to $M_Z/2$. The solid lines indicate FFs at LO and other lines show FFs at NLO. Our FF at LO agrees with Braaten's work [24] for j/ψ as shown in Fig. 8. The diagrams at LO and NLO indicate that the one-loop corrections enhance the FP to the $Q \to Q\bar{Q} + Q$ process. When the energy scale has been increased, it is observed that the FF enhances in the small z region. For any arbitrary value μ, we observed that the peak of NLO diagram become higher than LO diagram. Near the peak, for arbitrary value of initial quark squared energy 2μ, the NLO corrections enhance FP at least 16% for j/ψ and Υ respect to the lowest order near the peak at $\mu = 3m_Q$. This value grows by increasing the renormalization scale somewhat for

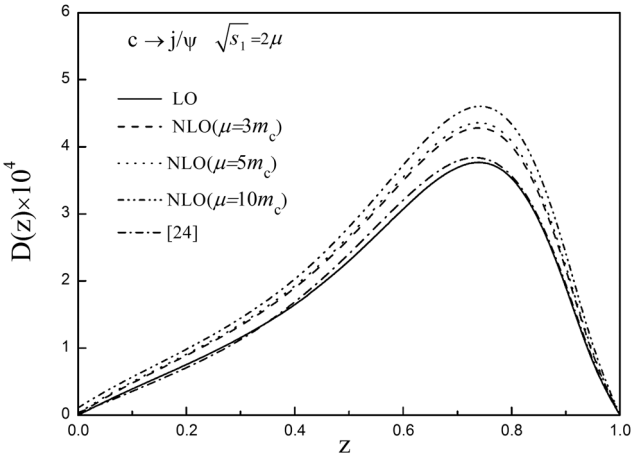

FIG. 8. The FF of c to j/ψ as a function of z. The solid line and dash-dot line indicate the FF at LO in our work and Ref. [24], respectively. The FFs at NLO have been shown in different values of the renormalization scale μ, from $3m_c$, $5m_c$, and $10m_c$ with dash, dot, and dash-dot-dot lines.

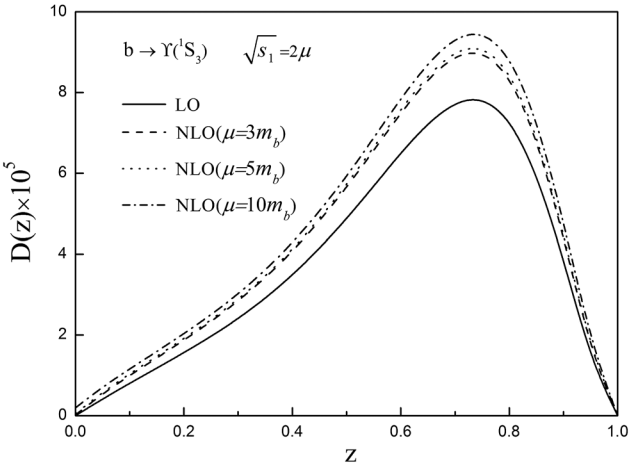

FIG. 9. The FF of b to Υ as a function of z. The solid line indicates FF at LO and the FFs at NLO are shown in different values of renormalization scale, for values $\mu = 3m_b$, $5m_b$, and $10m_b$ with dash, dot, and dash-dot lines, respectively.

$\mu = M_Z/2$, FP at NLO enhances by a factor of about 2 for the j/Ψ meson, and it grows more slowly by a factor of about 1.2 for the Υ meson. The mean value of the longitudinal momentum fraction, z is 0.7 at LO and NLO. In the Suzuki model [32] this parameter is about 0.7 for j/Ψ and 0.76 for Υ meson at LO, actually they are close together. This means produced heavy quarkonium in fragmentation process carry a large portion of longitudinal momentum fraction of initial quark. In another comparison, the FP in our work is larger than FP in Suzuki fragmentation model. This difference has been caused by adopting a different calculation method for the phase space. Both works have the same amplitude spinors and contain spin information. The Braaten perturbative model integrates over the invariant mass of the fragmenting quark [24], but in our work the integration is done over $k_T'^2$. In addition, we employed the above parameters in the perturbative FF obtained in Ref. [40]. There, the authors improved the FF obtained within the model Berger [41] by modifying the wave function but the FF at the Berger model works just for $z > 0.95$ and does not comply with predictions about the behavior of the FF at small z. However, we compare the FP with that work at LO because the FF is derived from the same Feynman diagram and the hadron momentum p is portioned equally between the constituents formed meson the same as our work. The result of Ref. [40] in Table I has been divided by a factor π. Actually, the FP at LO is larger than our result by a factor of 2.5 for the Υ and j/Ψ mesons. It should be noted that the Berger FF is obtained by integrating on the transverse momentum final state and it is obtained in the axial gauge and with no spin information.

We find that the FF at the NLO is sensitive to selection of the μ scale. The results show that QCD corrections to FFs have a significant effect on the production of quarkonium states at large transverse momentum. Generally, the NLO corrections can enhance FP and, thus, it can be used to calculate the hadron cross section and help to modify the quarkonium polarization theoretically. The infinitesimal disagreement between our result and the others listed in Tables I and II can be due to dependence of our FF on the value k_T' and the meson wave function effects, etc.

[1] J. J. Aubert *et al.*, Phys. Rev. Lett. **33**, 1404 (1974).
[2] D. C. Hom *et al.*, Phys. Rev. Lett. **39**, 252 (1997).
[3] T. Matsui and H. Satz, Phys. Lett. B **178**, 416 (1986).
[4] R. Aaij *et al.* (LHCb Collaboration), Eur. Phys. J. C **71**, 1645 (2011).
[5] R. Aaij *et al.* (LHCb Collaboration), Eur. Phys. J. C **72**, 2025 (2012).
[6] R. Aaij *et al.* (LHCb Collaboration), J. High Energy Phys. 02 (2013) 041.
[7] K. Aamodt *et al.* (ALICE Collaboration), Phys. Lett. B **704**, 442 (2011).
[8] B. Abelev *et al.* (ALICE Collaboration), Phys. Lett. B **718**, 295 (2012).
[9] B. Abelev *et al.* (ALICE Collaboration), J. High Energy Phys. 11 (2012) 065.
[10] G. Aad *et al.* (ATLAS Collaboration), Nucl. Phys. **B850**, 387 (2011).
[11] G. Aad *et al.* (ATLAS Collaboration), Phys. Rev. D **87**, 052004 (2013).
[12] V. Khachatryan *et al.* (CMS Collaboration), Phys. Rev. D **83**, 112004 (2011).
[13] S. Chatrchyan *et al.* (CMS Collaboration), J. High Energy Phys. 02 (2012) 011.
[14] S. Chatrchyan *et al.* (CMS Collaboration), Phys. Lett. B **727**, 101 (2013).
[15] R. Aaij *et al.* (LHCb Collaboration), J. High Energy Phys. 06 (2013) 064.
[16] E. Braaten, S. Fleming, and T. C. Yuan, Annu. Rev. Nucl. Part. Sci. **46**, 197 (1996).
[17] E. Braaten, arXiv:hep-ph/9702225.
[18] M. Beneke, arXiv:hep-ph/9703429.
[19] I. Z. Rothstein, arXiv:hep-ph/9911276.
[20] F. Maltoni, arXiv:hep-ph/0007003.
[21] E. L. Berger and D. Jones, Phys. Rev. D **23**, 1521 (1981).
[22] R. Baier and R. Rückl, Phys. Lett. **102B**, 364 (1981).
[23] G. T. Bodwin, E. Braaten, and G. P. Lepage, Phys. Rev. D **51**, 1125 (1995).

[24] E. Braaten, K. Cheung, and T. C. Yuan, Phys. Rev. D **48**, 4230 (1993).
[25] E. Braaten and T. C. Yuan, Phys. Rev. Lett. **71**, 1673 (1993).
[26] P. Artoisenet and E. Braaten, J. High Energy Phys. 04 (2015) 121.
[27] G. Xiangrui, J. Yu, L. LiuJi, and X. Xiaonu, arXiv:1606.07455.
[28] J. P. Ma, Phys. Lett. B **332**, 398 (1994).
[29] G. T. Bodwin and J. Lee, Phys. Rev. D **69**, 054003 (2004).
[30] Y. Q. Ma, J. W. Qiu, and H. Zhang. Phys. Rev. D **89**, 094029 (2014).
[31] R. Sepahvand and S. Dadfar,Nucl. Phys. **A848**, 218 (2010).
[32] M. Suzuki, Phys. Rev. D **33**, 676 (1986).
[33] J. C. Collins and D. E. Soper, Nucl. Phys. **B194**, 445 (1982).
[34] G. T. Bodwin, H. S. Chung, U-R. Kim, and J. Lee, Phys. Rev. D **91**, 074013 (2015).
[35] J. C. Romao, *Modern Techniques for One-Loop Calculations* (IST, 2004), http://porthos.ist.utl.pt/OneLoop/one-loop.pdf.
[36] T. Hahn, Comput. Phys. Commun. **140**, 418 (2001).
[37] R. Mertig, M. Bohm, and A. Denner, Comput. Phys. Commun. **64**, 345 (1991).
[38] J. Jiang, L. B. Chen, and C. F. Qiao, Phys. Rev. D **91**, 034033 (2015).
[39] B. W. Harris and J. F. Owens, Phys. Rev. D **65**, 094032 (2002).
[40] B. Z. Kopeliovich, H. J. Pirner, I. K. Potashnikova, I. Schmidt, and A. V. Tarasov, Phys. Rev. D **77**, 054004 (2008).
[41] E. L. Berger, Z. Phys. C **4**, 289 (1980).